Appendix 4 – Derivations

Derivation 1 - Fourier Heat Equation

We begin with the Fourier heat equation.

$$\frac{\partial U(x,y,z,t)}{\partial t} = a\nabla^2 T$$

Where U is the temperature of the sample at every point in space and time, *a* is a constant, and $\nabla^2 = \frac{\partial^2}{\partial x^2} + \frac{\partial^2}{\partial y^2} + \frac{\partial^2}{\partial z^2}$.

We could solve this equation for many geometries, but the simplest solution is for an infinite plane of material in the y, z directions with thickness L in the x direction. This reduces the problem to 1D and approximates a cast plate where the thickness is much smaller than the other two dimensions. The equation reduces to:

$$\frac{\partial U(x,t)}{\partial t} = a\frac{\partial^2}{\partial x^2}U .$$

Boundary conditions

1. Let us assume that the temperature of the mold is absolute zero so U(0,t) = U(L,t) = 0. This is a reasonable 0th order approximation if $T_g >> T_{mold}$ where T_g is the glass transition temperature where the liquid material becomes a glass, and T_{mold} is the temperature of the mold.
2. Let us assume that the temperature of the material when it is cast into the mold at t = 0 is U(x,0) = T_L or the liquidus temperature.

We must also assume that T(x,t) = T(t)X(x) so separation of variables applies. This gives

$$\frac{T'(t)}{aT(t)} = \frac{X''(x)}{X(x)} = -\lambda$$

The solutions for $\lambda \leq 0$ force U = 0 and for $\lambda > 0$ we find

$$T(t) = Ae^{-\lambda at}$$

and $X(x) = B\sin(x\sqrt{\lambda}) + C\cos(x\sqrt{\lambda})$ where $\lambda = n\pi / L$

Applying boundary conditions gives

$$U(x,t) = \sum_{n=1}^{\infty} D_n \left(\sin\frac{n\pi x}{L}\right) e^{-\frac{n^2\pi^2 at}{L^2}}$$

Where $D_n = \frac{2}{L}\int_0^L T_L \sin\left(\frac{n\pi x}{L}\right)dx = T_L\frac{2-2\cos(n\pi)}{n\pi}$

The critical cooling rate is the time required to cool the centerline to T_g.

Critical cooling rate = U(L/2,t)=T_g.

$$T_g = T_L \sum_{n=1}^{\infty} \frac{2 - 2\cos(n\pi)}{n\pi} \sin\left(\frac{n\pi}{2}\right) e^{-\frac{n^2\pi^2 at}{L^2}}$$

We can solve this for n = 1 for the first order approximation and find that

$$t = \frac{L^2}{\pi^2 a} \ln \frac{T_L}{T_g}$$

The important message from this derivation is that the critical cooling rate goes like the thickness squared (L^2).

Derivation 2 - Implications of Slope Change in Thermodynamic Variables

Assume a slope change in the entropy S(T) or enthalpy H(T) of a material. Call the temperature where the slope change occurs T_g. We know from thermodynamics that

$$c_V = T\left(\frac{\partial S}{\partial T}\right)_V \text{ and } c_P = T\left(\frac{\partial S}{\partial T}\right)_P = \left(\frac{\partial H}{\partial T}\right)_P$$

If either H or S changes slope at T_g then

$$\left(\frac{\partial S(T_g^{+})}{\partial T}\right)_V \neq \left(\frac{\partial S(T_g^{-})}{\partial T}\right)_V \text{ and } \left(\frac{\partial S(T_g^{+})}{\partial T}\right)_P \neq \left(\frac{\partial S(T_g^{-})}{\partial T}\right)_P$$

and we would expect a discontinuous c_V and c_P. Similarly if the slope of P(T) changes at T_g then we would expect discontinuities in the compressibility. These slope changes are observed in glass forming liquids and the discontinuities in c_P as measured in a DSC provide a way to determine the glass transition temperature.

Derivation 3 - Stephan's Equation for Parallel Plate Viscometer

The viscosity equation for a parallel plate viscometer geometry is called Stefan's Equation. It is solved fully in "Theory and Application of the Parallel Plate Plastometer" [G.J. Dienes, H.F. Klemm, J. Appl. Phys. 17 (1946) 458]. The derivation takes four journal pages and the basic strategy is given here.

Begin with the equation of motion for a viscous fluid. Neglect body forces. Transform to cylindrical coordinates and consider a cylinder with height << radius. Assume no slippage at the plates and a parabolic flow front.

General expression for motion of a Newtonian fluid of viscosity η neglecting body forces is

$$\rho \frac{d\vec{v}}{dt} + \rho \vec{v} \bullet \nabla \vec{v} = -\nabla p + \eta \nabla^2 \vec{v} + \frac{1}{3} \eta \nabla \nabla \bullet \vec{v}$$

assuming incompressibility requires $\nabla \bullet \vec{v} = 0$

assuming velocity is small we neglect $\rho \vec{v} \bullet \nabla \vec{v}$

and are left with $\rho \frac{d\vec{v}}{dt} = -\nabla p + \eta \nabla^2 \vec{v}$

In cylindrical coordinates we have three equations

$$\rho \frac{dv_r}{dt} = -\frac{d\rho}{dr} + \eta \nabla^2 v_r$$

$$\rho \frac{dv_\theta}{dt} = -\frac{1}{r} \frac{d\rho}{d\theta} + \eta \nabla^2 v_\theta$$

$$\rho \frac{dv_z}{dt} = -\frac{d\rho}{dz} + \eta \nabla^2 v_z$$

The parallel plates are located at z = 0 and z = h

circular symmetry requires $v_\theta = 0$

assuming a short sample lets us assume $v_z \sim 0$

assuming no slippage and steady state flow means

$$v_r(z = 0) = v_r(z = h) = 0 \text{ and } \frac{dv_r}{dt} = 0$$

ASSUMPTIONS ARE GREAT!!!!!! We are left with

$$\frac{d\rho}{dr} = \eta \frac{d^2 v_r}{dz^2}$$

Integrate twice and apply the boundary conditions

$$v_r = \frac{1}{2\eta} \frac{dp}{dr} (z - h) z$$

consider flow through a surface element $r\,d\theta\,dz = r\,d\theta\,dz\,v_r$

$$U = \text{flow per unit arclength} = \int_0^h v_r \, dz = \frac{1}{2\eta} \frac{dp}{dr} \int_0^h z^2 - z h \, dz$$

$$U = -\frac{h^3}{12\eta} \frac{dp}{dr}$$

next we let the plates move towards eachother at a rate $\frac{dh}{dt}$

a volume element $r\,dr\,d\theta\,dz$ changes volume at a rate $r\,dr\,d\theta \frac{dh}{dt}$

since the fluid is incompressible the rate of decrease of volume must equal the outward flow rate. Thus,

$$-r\,dr\,d\theta \frac{dh}{dt} = \frac{\partial}{\partial r} (r\,d\theta\,U)\,dr \rightarrow \frac{12\eta}{h^3} \frac{dh}{dt} r = \frac{\partial}{\partial r} \left(r \frac{\partial p}{\partial r} \right)$$

Integrating and requiring that p is finite for r = 0 and p(r = R) = atmospheric pressure gives

$$p = -\frac{3\eta}{h^3} \frac{dh}{dt} \left(R^2 - r^2 \right) + 1\,\text{atm}$$

We must balance the forces on the plate in steady state flow.

$$\text{Downward force applied to top plate} = F + \int_0^R 1\,\text{atm} * 2\pi r\,dr$$

$$\text{Sample applies this force upwards} = \int_0^R p\,2\pi r\,dr$$

$$\text{We arrive at } F = -2\pi \frac{dh}{dt} \frac{3\eta}{h^3} \int_0^R \left(R^2 - r^2\right) r\,dr$$

solving for the case where radius of plate (R) = radius of sample (a)we obtain

$$F = -\frac{3\pi\eta a^4}{2h^3} \frac{dh}{dt}$$

Solving for the case where we assume the plates are larger than the diameter of the cylinder we are squishing and we find:

$$F = \frac{-3\eta V^2}{2\pi h^5} \frac{dh}{dt}$$

Where F is the applied force, η is the viscosity, V is the volume, h is the height, dh/dt is the time derivative of the height of the specimen which is assumed to be incompressible.

Derivation 4 – Vogel-Fulcher-Tammann Viscosity

Some liquids are observed to exhibit Arrhenius type behavior. This means that their flow properties as a function of temperature can be well described by

$\eta(T) = \eta_0 e^{\frac{T_0}{T - T_0}}$ where η_0 is the high temperature viscosity limit $\approx 10^{-5}$ Pa-s, and T_0 is the temperature at which no flow occurs. Deviations from this behavior are observed for many liquids. The deviation usually results in a steeper drop of viscosity with temperature than the Arrhenius relationship predicts. This is called hyper-Arrhenius behavior. To allow for this, the Vogel-Fulcher-Tammann (VFT) fit to the viscosity data has a multiplier in the exponent as seen below.

$$\eta = \eta_0 \exp^{\frac{D^* T_0}{T - T_0}}$$

where D^* is a fitting constant and η_0 and T_0 are defined as before. T_0 is also called the VFT temperature.

Derivation 5 - Viscosity of BMG from Potential Energy Landscape Perspective

Flow of a metallic glass is described as barrier crossing events in "Rheology and Ultrasonic Properties of Metallic Glass-Forming Liquids" published in Materials Research Society Bulletin [W.L. Johnson, M.D. Demetriou, J.S. Harmon, M.L. Lind, K. Samwer, MRS Bull. 32 (2007) 644].

A barrier to flow is argued to be a function of STZ volume (Ω(T, P)) and the energy barrier to shear flow of the STZ which is shear modulus (G(T, P)). The total barrier to flow is W~G*Ω. The barrier to flow at the glass transition temperature is W_g.

Experimental data suggests that the contributions of the shear modulus and STZ volume barriers are similar and can be well represented by

$$W = W(G(T), \Omega(T)) = W_g \left(\frac{T_g}{T}\right)^n \left(\frac{T_g}{T}\right)^p$$

$$W \sim W_g (T_g/T)^{2n}$$

Taking the barrier crossing rate normalized by an attempt frequency to follow a Boltzmann distribution (equivalently, thermally activated hopping), one arrives at a viscosity law that takes the form

$$\frac{\eta}{\eta_\infty} = \mathrm{Exp}[-W/kT]$$

Because these flow barriers give rise to the observed viscosity, The exponents are shown to be related to the fragility as follows.

$$m = (1+2n)\,\mathrm{Log}(\eta_g/\eta_\infty)$$

where

$$m = \left(\frac{\partial\, \mathrm{Log}\eta}{\partial\,(T_g/T)}\right)_{T_g=T}$$

and

$$W_g = kT_g \ln(\eta_g/\eta_\infty).$$

We can combine terms

$$\frac{\eta}{\eta_\infty} = \mathrm{Exp}\left[\frac{W_g}{kT}\left(\frac{T_g}{T}\right)^{2n}\right]$$

$$\mathrm{Ln}\left[\frac{\eta}{\eta_\infty}\right] = \frac{W_g}{kT}\left(\frac{T_g}{T}\right)^{2n} \quad \text{solve for } T_g$$

$$\mathrm{Ln}\left[\frac{\eta_g}{\eta_\infty}\right] = \frac{W_g}{kT_g}\left(\frac{T_g}{T_g}\right)^{2n} \rightarrow W_g = K T_g \mathrm{Ln}\left[\frac{\eta_g}{\eta_\infty}\right] \quad \text{plugging back in}$$

$$\mathrm{Ln}\left[\frac{\eta}{\eta_\infty}\right] = \mathrm{Ln}\left[\frac{\eta_g}{\eta_\infty}\right]\left(\frac{T_g}{T}\right)^{2n+1}$$

$$\mathrm{Log}\left[\frac{\eta}{\eta_\infty}\right] = \frac{\mathrm{Ln}\left[\frac{\eta_g}{\eta_\infty}\right]}{\mathrm{Ln}[10]}\left(\frac{T_g}{T}\right)^{m/\mathrm{Log}(\eta_g/\eta_\infty)}$$

If we let

$$A = \mathrm{Log}(\eta_g/\eta_\infty)$$

we arrive at the expression

$$\mathrm{Log}\left[\frac{\eta}{\eta_\infty}\right] = A\left(\frac{T_g}{T}\right)^{m/A}$$

Derivation 6 - Thermoplastic Formability Parameter

Starting with the result of Derivation 5: $$\mathrm{Log}\left[\frac{\eta}{\eta_\infty}\right] = A\left(\frac{T_g}{T}\right)^{m/A}$$

We integrate as shown in Figure A4.1 by oversimplifying BMG physics and assuming all BMG exhibit the same viscosity at T_x.

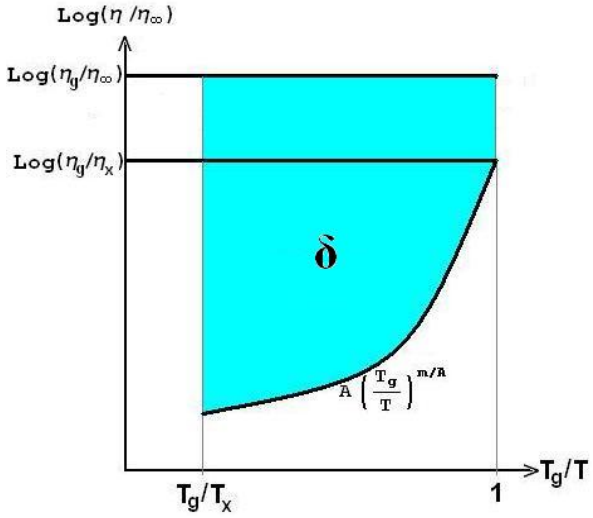

Figure A4.1: Thermoplastic formability parameter δ found by integrating as shown.

In reality, the square region may be different from alloy to alloy.

$$\delta = \int_{T_g/T_x}^{1} [A - \mathrm{Log}\,(\eta/\eta_\infty)]\, d\,(T_g/T)$$

$$\delta = \int_{T_g/T_x}^{1} \left[A - A\left(\frac{T_g}{T}\right)^{m/A}\right] d\,(T_g/T)$$

$$\delta = A\left(1 - \frac{T_g}{T_x}\right) - \frac{A}{1+\frac{m}{A}}\left[1 - \left(\frac{T_g}{T_x}\right)^{1+m/A}\right]$$

Squish data and correlation with δ are detailed in Figure A4.2.

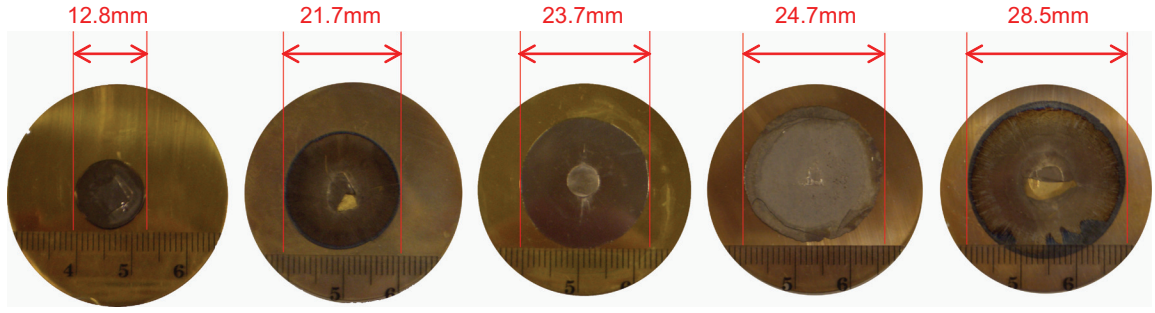

Figure A4.2: Squish test data for 5 TPF candidate alloys shows δ is a decent predictor of TPF potential.

Derivation 7 - Composition Counting

To determine the number of compositions one must create for 1 - 5 element alloys assuming 5% composition steps. There is a constraint that the sum of the elements = 100.

One element: There is only one choice with 100% of that element.

Two elements: Give the alloys shown in Table A4.1.

Table A4.1: All possible two component compositions with 5% composition steps.

Alloy #	1	2	3	4	5	6	7	8	9	10	11	12	13	14	15	16	17	18	19	20	21
%element1	100	95	90	85	80	75	70	65	60	55	50	45	40	35	30	25	20	15	10	5	0
%element2	0	5	10	15	20	25	30	35	40	45	50	55	60	65	70	75	80	85	90	95	100

We see 21 possible compositions.

Three elements: This case is best thought of with a ternary phase diagram as shown in Figure A4.3. This can be drawn in 2D because of the constraint that the sum of the elements = 100. The alloy's composition is determined by drawing lines orthogonal to the corners. In the Ti corner, the alloy would have 100% Ti. Horizontal lines orthogonal to the Ti corner are drawn in 5% composition steps. The lines slanting downward are drawn orthogonal to the Be corner in 5% composition steps. Intersections of the lines form a grid in the triangle where the Zr composition = 100 – Ti – Be. There are 21 compositions along the bottom of the triangle going from the Be corner to the Zr corner with Ti = 0%. There are 20 compositions possible along the line Ti = 5% just above the bottom of the triangle. This continues until we reach the Ti corner with 1 possible composition. The total number of compositions is 21 + 20 + 19 + . . . + 2 + 1 = 231.

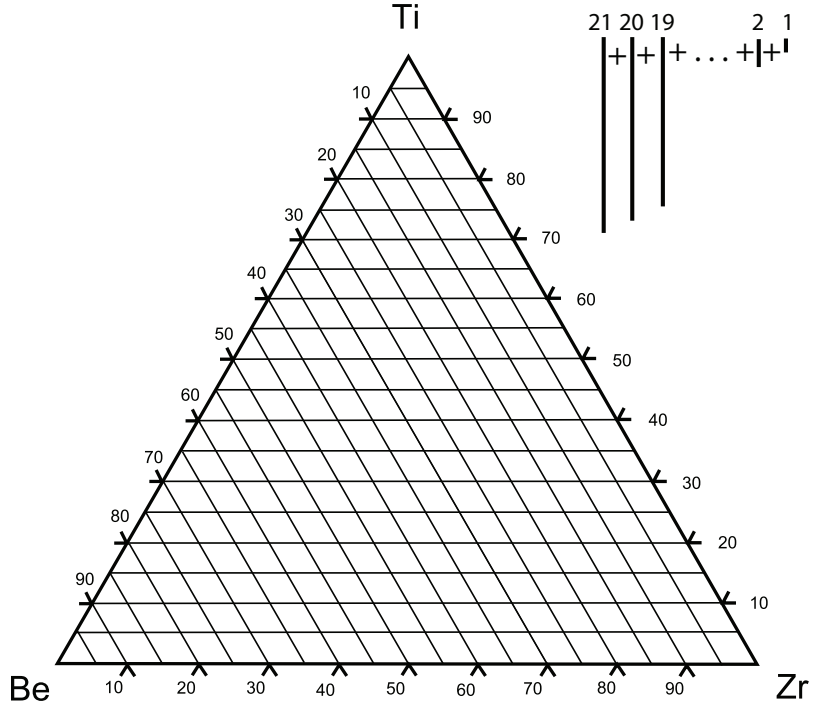

Figure A4.3: All possible three component compositions with 5% composition steps found at line intersections.

Four elements: This case is best approached with a quaternary phase diagram drawn in 3D because of the constraint as shown in Figure A4.4. In this case the phase diagram is an equilateral pyramid with compositions determined by a plane orthogonal to each corner. Instead of adding line elements, we add equilateral triangle elements as shown below. A table with the math is included after the 5 element analysis.

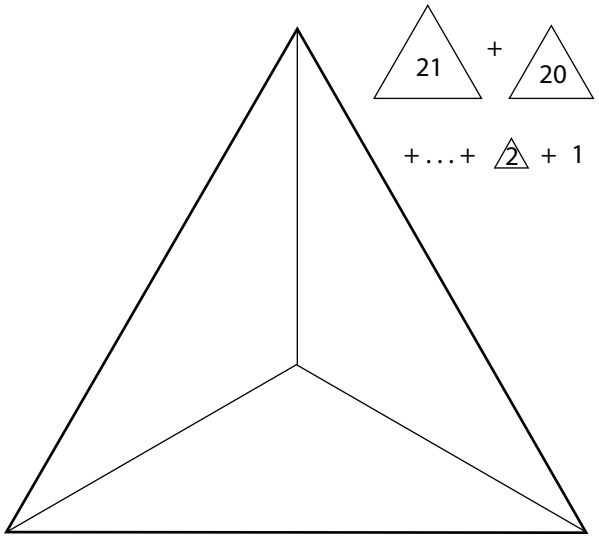

Figure A4.4: Four component phase diagram is an equilateral pyramid / tetrahedron.

Five elements: This case can't be drawn and occupy a 4D phase diagram that is an equilateral hyperpyramid as shown in Figure A4.5. Instead of adding equilateral triangles for composition steps, we now add equilateral pyramid elements shrinking in size as shown below. The counting follows.

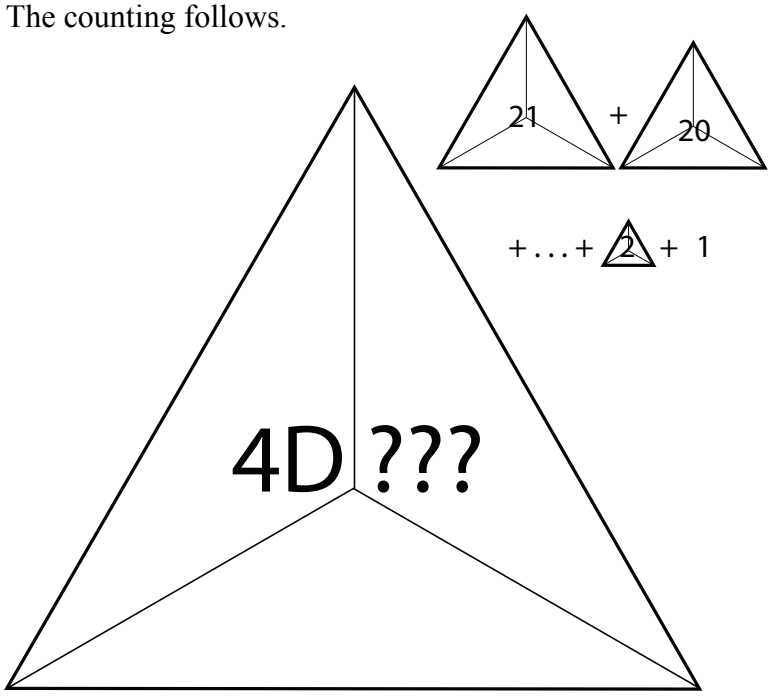

Figure A4.5: Five component phase diagram is a 4D equilateral hyperpyamid.

The 3 element phase diagram compositions were counted using an additive factorial type function which we will define as !:.The combinatorics are shown in Table A4.2.

3 element = 21!: = 21 + 20 + 19 + . . . + 2 + 1 = 231
4 element = 21!: + 20!: + 19!: + . . . + 2!: + 1 = 1771
5 element = 4 element(21) + 4 element(20) + . . . + 4 element(2) + 1 = 10626

Table A4.2: Combinatorics for 3 - 5 element alloys.

																							1	1	1
																						2	1	3	1
																					3	2	1	6	1
																				4	3	2	1	10	1
																			5	4	3	2	1	15	1
																		6	5	4	3	2	1	21	1
																	7	6	5	4	3	2	1	28	1
																8	7	6	5	4	3	2	1	36	1
															9	8	7	6	5	4	3	2	1	45	1
														10	9	8	7	6	5	4	3	2	1	55	1
													11	10	9	8	7	6	5	4	3	2	1	66	1
												12	11	10	9	8	7	6	5	4	3	2	1	78	1
											13	12	11	10	9	8	7	6	5	4	3	2	1	91	1
										14	13	12	11	10	9	8	7	6	5	4	3	2	1	105	1
									15	14	13	12	11	10	9	8	7	6	5	4	3	2	1	120	1
								16	15	14	13	12	11	10	9	8	7	6	5	4	3	2	1	136	1
							17	16	15	14	13	12	11	10	9	8	7	6	5	4	3	2	1	153	1
						18	17	16	15	14	13	12	11	10	9	8	7	6	5	4	3	2	1	171	1
					19	18	17	16	15	14	13	12	11	10	9	8	7	6	5	4	3	2	1	190	1
				20	19	18	17	16	15	14	13	12	11	10	9	8	7	6	5	4	3	2	1	210	1
		21		20	19	18	17	16	15	14	13	12	11	10	9	8	7	6	5	4	3	2	1	231	1
																								Sum line	
																								Sum pyramid	
																								Sum Hyperpyramid	

Derivation 8 - Limiting Cases of Two Phase Liquid Flow

A recent study of amorphous alloys in the ZrTiBe system showed the possibility of a miscibility gap in the supercooled liquid region along the Be = 40 pseudo binary line, but no microscopic evidence of the two phases was obtained. The two phase glasses are thought to separate into a Zr rich phase with a glass transition temperature $T_{g1} \sim 320$ °C and a Ti rich phase with $T_{g2} \sim 375$ °C. If there are indeed two glasses, one would expect to see flow, or more precisely viscosity, as a function of temperature characteristic of a two phase liquid.

The flow of liquids with multiple phases was a phenomenon studied extensively in the early 1900s. Two limiting cases were solved for ideal mixtures. Variations of these ideal cases were postulated to explain the flow of other types of liquid mixtures. Both cases consider a liquid mixture with parallel layers or laminae. The applied shear stress is orthogonal to the layers in Case 1 as shown in Figure A4.6. The applied shear stress is parallel to the layers in Case 2 as shown in Figure A4.7.

The fundamental law governing viscous flow is

$$\frac{dv}{dr} = \frac{F}{\eta} \quad (1)$$

Where F is the applied shear stress, η is the viscosity, and $\frac{dv}{dr}$ is the spatial derivative of the velocity orthogonal to the shear direction.

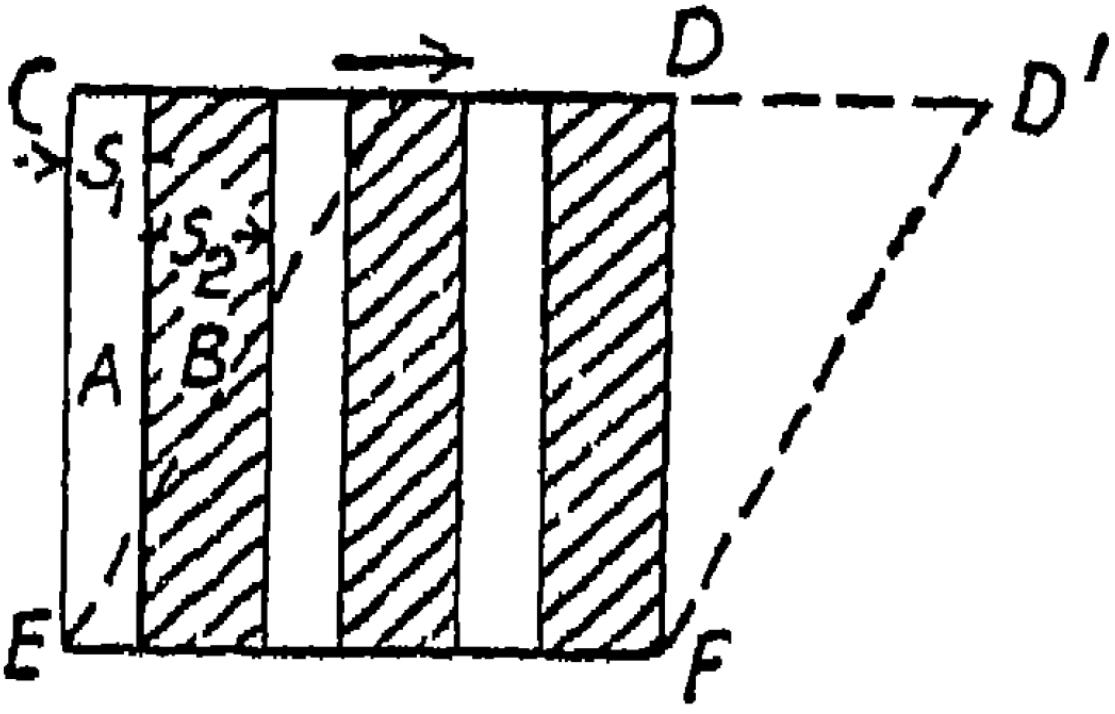

Figure A4.6: Case 1 showing laminae of two fluids orthogonal to shear direction.

Case 1 constrains the layers to have the same velocity. For simplicity consider a liquid with alternating laminae A, B, . . . with viscosities η_A and η_B . . ., and laminae thicknesses s_A and s_B . . ., and shear stresses per unit area P_A and P_B . . . Since we are considering only a simple shear stress, we can integrate equation 1 and find

$$v = \frac{RP}{H} = \frac{RP_A}{\eta_A} = \frac{RP_B}{\eta_B}$$

Where R is the distance between horizontal planes, H is the viscosity of the mixture, and P is the average shear stress over the entire distance S. $PS = P_A s_A + P_B s_B + \ldots$ Hence

$$H = \frac{R}{v}\left(\frac{P_A s_A + P_B s_B + \ldots}{S}\right)$$

Because s_A/S is the fraction by volume of substance A in the mixture, we can use the volume fraction c_i for the ith substance in the mixture and find viscosities are additive for Case 1.

$$H = \sum_i c_i \eta_i \quad (2)$$

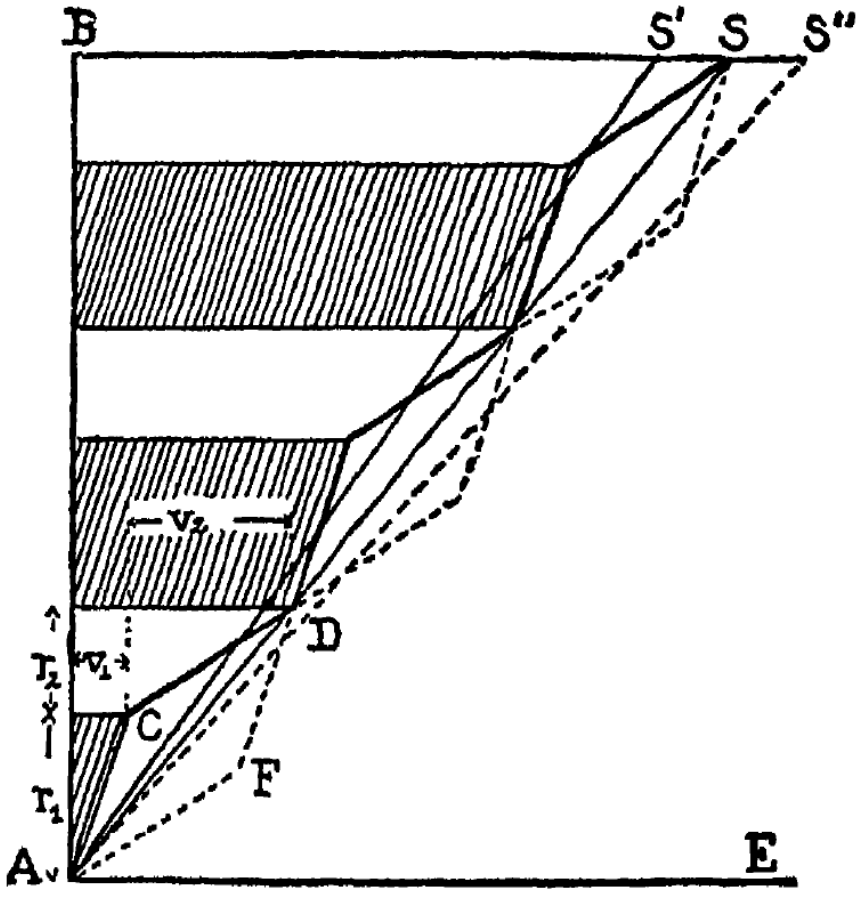

Figure A4.7: Case 2 showing laminae of two fluids parallel to shear direction.

The constraint in Case 2 requires the shearing stress to be constant across the layers such that

$$P = \frac{\eta_A v_A}{r_A} = \frac{\eta_B v_B}{r_B} = \ldots (3)$$

where the v_A and v_B are the partial velocities, and r_A and r_B are the thicknesses of the A and B laminae. The measured viscosity may be determined by the velocity of the top plane relative to the bottom one such that

$$P = \frac{Hv}{R} \quad (4).$$

The partial velocities of each layer are additive and combining equations 3 and 4 gives

$$\frac{PR}{H} = \sum_i v_i = \sum_i \frac{\Pr_i}{\eta_i}.$$

Substituting in the fluidity, Φ, which is defined to be the $1/\eta$, we find that

$$PR\Phi = P(r_A\phi_A + r_B\phi_B + \ldots).$$

But r_A/R is the volume fraction of substance A in the mixture and can be replaced by c_i. We find that fluidities are additive in Case 2.

$$\Phi = \sum_i c_i\phi_i \quad (5)$$

A similar derivation can be found in [1]. In immiscible fluids, the layers A and B resist indefinite extension and flow resembling Case 1 results. See page 87 of [1].

In the two phase amorphous $(Zr_aTi_{1-a})_{60}Be_{40}$ alloys, one would expect to see three regions of flow. The first region is at temperatures below T_{g1} where the sample would behave like a solid and little or no flow would be observed. The second region covers the temperature range $T_{g1} < T < T_{g2}$. In region 2, we should see a slope change in the viscosity versus temperature curve as the liquid-solid solution begins flow. The third region spans the temperature range $T_{g2} < T < T_x$. In region three, the sample should exhibit flow characteristic of a two phase liquid. At T_x the sample begins to crystallize and flow stops.

It is difficult to predict the flow properties of the $(Zr_aTi_{1-a})_{60}Be_{40}$ system in a quantitative manner. First we don't know the fragilities of the phases in the alloys. These will be assumed similar to Vitreloy type alloys with m = 40. Also, the flow in region 2 depends not only on volume fraction of the solid phase, but also the size distribution, which is unknown. There are many theoretical models predicting measured viscosity of a liquid solid mixture with known viscosity and solid phase fraction, but they vary by orders of magnitude in their predictions [2]. They are not presented here. A schematic picture of flow is desired. As such, the Johnson viscosity model [3] will be used and a solid will be assumed to have a viscosity = 10^{12} Pa-s. At T_{g1}, the first phase is assumed to soften and at T_{g2}, the second phase is assumed to soften and flow according to the Johnson model.

We will assume T_g values measured in the DSC are correct and also assume a fragility of 40 which is reasonable for Vitreloy type alloys.

We will look at flow predicted by both Case 1 and Case 2 for a glass similar to $Zr_{30}Ti_{30}Be_{40}$ with about 60% of the low T_g phase. Assume T_{g1} = 310 °C, T_{g2} = 360 °C, m = 40.

Case 1: Additive viscosities:

Region 1: $\eta(T < 310\ °C) = 0.6*10^{12} + 0.4*10^{12})$Pa-s

Region 2: $\eta(310\ °C < T < 360\ °C) = \left(0.6 * \eta_\infty * 10^{A\left(\frac{310}{T}\right)^{m/A}} + 0.4 * 10^{12} \right)$ Pa-s

Region 3: $\eta(360\ °C < T < T_x) = \left(0.6 * \eta_\infty * 10^{A\left(\frac{310}{T}\right)^{m/A}} + 0.4 * \eta_\infty * 10^{A\left(\frac{360}{T}\right)^{m/A}} \right)$ Pa-s

These equations are taken from the final equation of derivation 5 and solved for η.

Case 2: Additive fluidities so $\frac{1}{\eta} = \phi = c_1\phi_1 + c_2\phi_2 = \frac{c_1}{\eta_1} + \frac{c_2}{\eta_2}$

Solving for η gives $\eta = \frac{\eta_1 * \eta_2}{c_1\eta_1 + c_2\eta_2}$

Region 1: $\eta(T < 310\ °C) = \left(\frac{10^{12} * 10^{12}}{0.6 * 10^{12} + 0.4 * 10^{12}} \right)$ Pa-s = 10^{12} Pa-s

Region 2: $\eta(310\ °C < T < 360\ °C) = \left(\frac{\eta_\infty * 10^{A\left(\frac{310}{T}\right)^{m/A}} * 10^{12}}{\left(0.6 * \eta_\infty * 10^{A\left(\frac{310}{T}\right)^{m/A}} + 0.4 * 10^{12} \right)} \right)$ Pa-s

Region 3: $\eta(360\ °C < T < T_x) = \left(\frac{\eta_\infty * 10^{A\left(\frac{310}{T}\right)^{m/A}} * \eta_\infty * 10^{A\left(\frac{360}{T}\right)^{m/A}}}{\left(0.6 * \eta_\infty * 10^{A\left(\frac{310}{T}\right)^{m/A}} + 0.4 * \eta_\infty * 10^{A\left(\frac{360}{T}\right)^{m/A}} \right)} \right)$

The two limiting cases for two phase liquid flow are plotted in Figure A4.8.

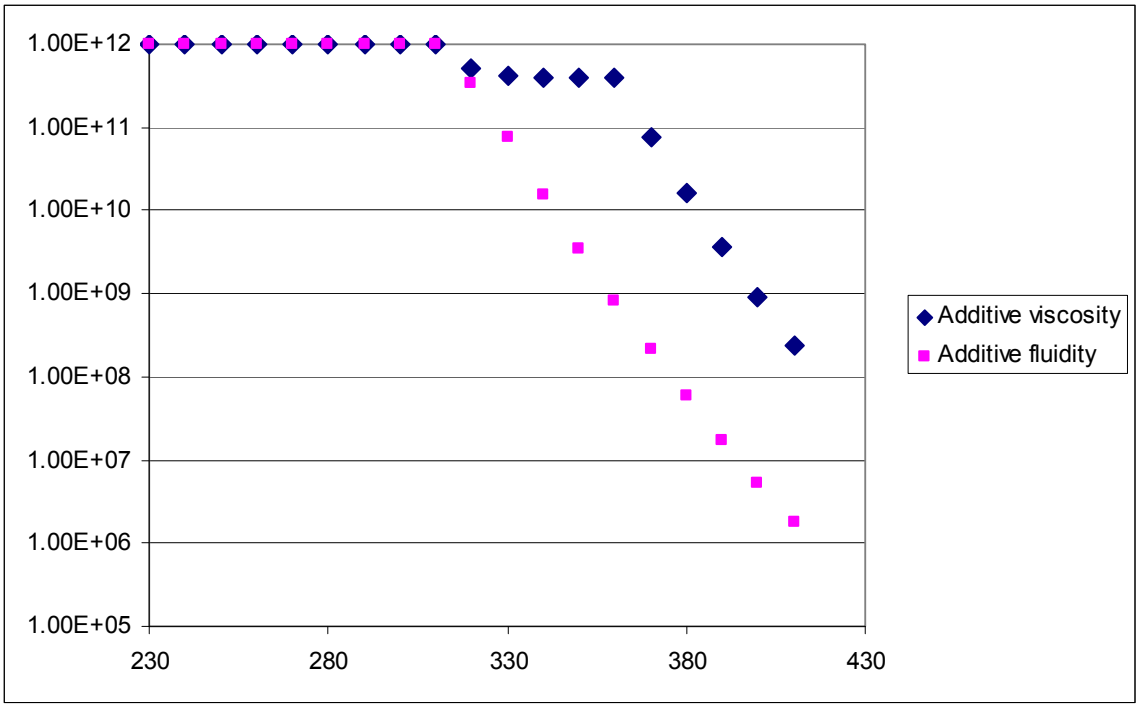

Figure A4.8: Additive fluidity cases and additive viscosity cases on three flow regions of a glass with 60% low T_g phase are shown. It is interesting to note that the theoretical additive viscosity case resembles the flow seen in figure 6.5 suggesting that we may approach the immiscible fluids resisting indefinite extension case proposed in [1] on page 87.

Derivation 9 - Modulus of Rupture Equation for Rectangular Beam

Modulus of Rupture for beam bending

$$\sigma = \frac{M * y}{I} = \frac{3 * F * L}{2 * b * h^2}$$

Where
σ = stress parallel to neutral axis
M = bending moment
y = distance from neutral axis
I = second moment of area

We begin by considering a strain in the x direction which is related to the distance from the neutral axis as follows

$$\epsilon_x = -\kappa y$$

The resulting stress is

$$\sigma_x = E \epsilon_x = -E \kappa y$$

$$dM = -\sigma_x y\, dA$$

$$M = \int E\kappa y^2\, dA$$

$$I = \int y^2\, dA = \int_{-b/2}^{b/2}\int_{-h/2}^{h/2} y^2\, dy\, dz$$

$$I = \frac{bh^3}{12}$$

$$M = E\kappa I = \frac{\sigma_x I}{y}$$

$$\sigma_{xmax} = \frac{My}{I} = \frac{\frac{F}{2} * \frac{L}{2} * \frac{h}{2}}{\frac{bh^3}{12}} = \frac{3FL}{2bh^2}$$

Appendix 4 References

[1] E.C. Bingham, Fluidity and Plasticity, McGraw-Hill Book Company, Inc., Ohio, 1922, pp. 81-105.

[2] C. Journeau, G. Jeulain, L. Benyahia, J.F. Tassin, P. Abélard, Rhéologie 9 (2006) 28.

[3] W.L. Johnson, M.D. Demetriou, J.S. Harmon, M.L. Lind, K. Samwer, MRS Bull. 32 (2007) 644.